焊接应力变形原理若干问题的探讨(一)

王者昌
(中国科学院 金属研究所, 沈阳 110016)

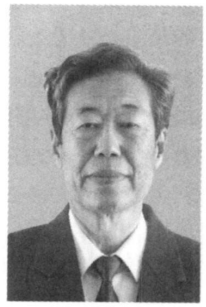

王者昌

摘 要: 在焊接加热和冷却过程中, 组成焊件的小窄条之间不可能存在完全刚性拘束, 端面不可能保持平面, 会分别产生凸出和凹进, 平截面假设不成立。不用平截面假设也可以得到类似的焊接残余应力分布。焊缝不存在残余压缩塑性应变, 只存在拉伸应变, 焊缝和近缝区残余压缩塑性应变分布和大小的传统观点不成立。提出新的近似用熔池最宽处温度分布表示的拉伸塑性应变分布原理图及其相应的计算公式。

关键词: 焊接应力应变; 平截面假设; 压缩塑性应变; 拉伸塑性应变
中图分类号: TG404 文献标识码: A 文章编号: 0253-360X(2008)06-0073-04

0 序 言

一般认为, 焊缝和近缝区存在残余拉应力, 两侧则存在与其平衡的压应力。残余拉应力的存在可能引起焊接冷裂纹、结构脆断、应力腐蚀开裂和疲劳寿命降低等不良后果, 压应力则可能导致薄壳结构失稳翘曲变形, 从而影响焊接质量[1]。20 世纪 30 年代以来焊接应力变形问题一直受到人们的关注[2,3]。为分析焊接应力变形, 奥凯尔勃洛姆[3] 提出了平截面假设, 关桥对平截面假设提出质疑; 传统观点认为焊缝存在压缩塑性应变和残余压缩塑性应变[4-8]; 而文献[9—11] 则认为焊缝不存在压缩塑性应变; 文献[6] 认为, 残余压缩塑性应变应示为 B_0KKB_0。残余压缩塑性应变为加热时产生的压缩塑性应变与冷却时产生的拉伸塑性应变之差, 文献[11] 认为两者之差不应该是 B_0KKB_0。可以看出, 上述诸问题还没有统一认识, 进行深入讨论是必要的。以下讨论薄板单道焊焊接纵向应力应变相关问题。由于要讨论的问题较多, 受篇幅所限, 每篇文章只能讨论 2~3 个问题, 故将分成若干篇文章进行讨论。

1 关于平截面假设

在分析板材焊接应力变形时, 板材可看作由若干互不相连的小窄条组成, 若每根小窄条都可按自己被加热或冷却到的温度自由变形, 则板条的端面应为与温度相对应的曲面。实际上, 组成板材的小窄条之间互相约束。假设板端面始终保持平面, 在焊接加热过程中, 金属受热膨胀, 板端面平移, 产生伸长应变 Δ, 在冷却过程, 降温收缩, 板端面平移, 产生缩短应变 Δ_l, 形成了如图 1[3] 所示的应力应变分布, 图中 d 为缩短应变宽度。上述平截面假设对于只掌握材料力学知识的人在分析焊接应力变形时是有帮助的。但实际上, 上述小窄条之间的约束不是完全刚性的, 端面不可能保持平的。1963 年关桥在其研究生学位论文中就指出平截面假设的不足: "如

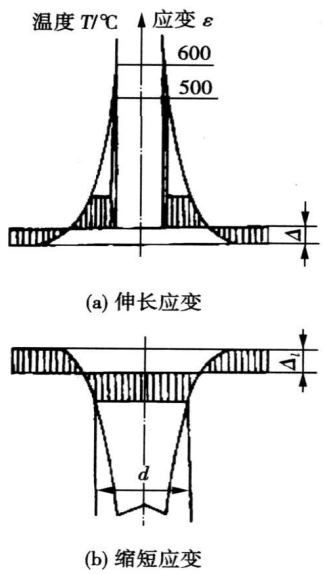

图 1 在平板上堆焊时的应力应变

Fig. 1 Stress-strain distribution of steel plate during surfacing

收稿日期: 2007-03-13

果钢焊接时平截面假设在其计算残余应力值方面的缺点被钢的较大收缩塑性变形储备所掩盖的话，那么对钛而言，平截面假设造成的计算残余应力值大大高于试验值”。在此，关桥指出平截面假设对钛合金不适用，但未否定对低碳钢的适用性。

在焊接加热时，热源前方的金属受热膨胀，组成板材的小窄条由于互相约束，不能完全自由膨胀，只能部分膨胀，焊件中部产生凸出，另一部分则引起应力和应变（包括弹性应变和塑性应变），板中部产生压应力和压应变，两侧则为拉应力和拉应变。板边端面产生伸长的位移 ΔA，如图 2 所示。同样，在冷却过程中，板条降温收缩因互相约束不能完全进行，即只能部分收缩，焊件中部产生凹进，另一部分则引起应力和应变，平截面假设不成立。板中部产生拉应力和拉应变（包括弹性拉伸应变和塑性拉伸应变），两侧为压应力和压应变，板边端面产生缩短的位移 ΔB（$\Delta B > \Delta A$），如图 2 所示。可以看出，不用平截面假设，照样可得到类似图 1 所示的应力应变分布。

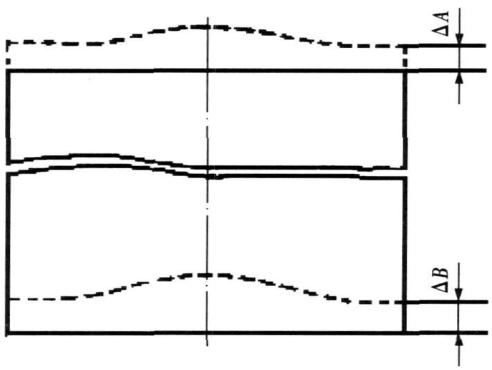

图 2 平板焊接时的变形

Fig 2 Deformation of plate during welding

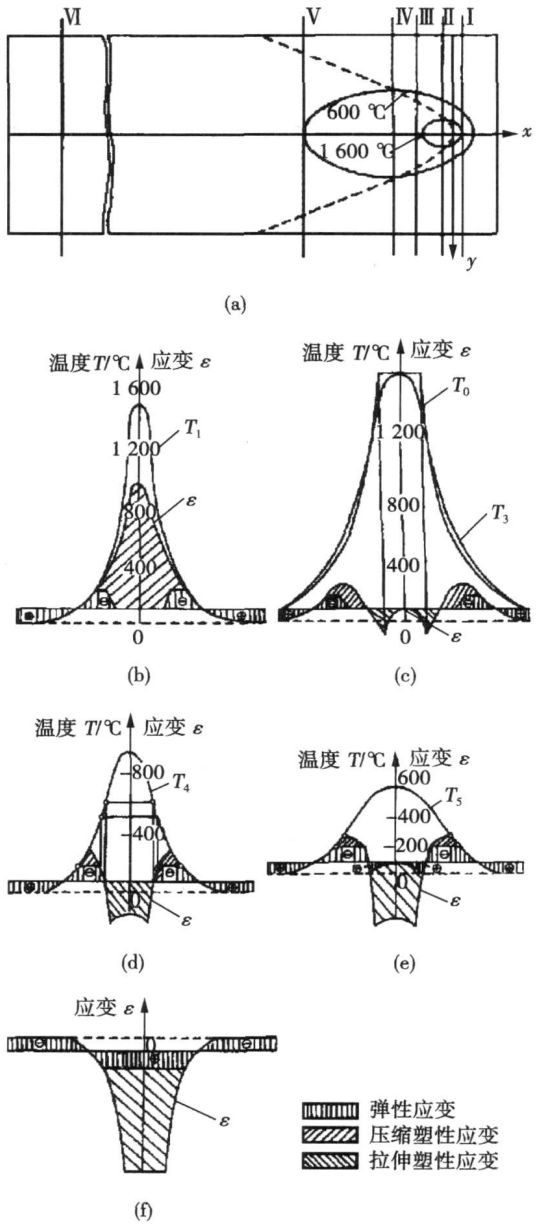

图 3 低碳钢板焊接时温度场和应力应变分布

Fig 3 Temperature and stress-strain distribution during welding of low carbon steel

2 焊接应力应变发展过程

如图 3 所示的焊接应力应变发展过程，作者在文献[11] 中已做了比较详细的介绍，这里对应力应变过程只做简单说明。

断面Ⅰ取自熔池前沿，中心区升温高于两侧金属，其膨胀受阻产生压应力和压应变，两侧金属产生拉应力和拉应变，应力应变分布如图 3b 所示。

文献[12] 将焊缝定义为：“焊件焊接后形成的结合部分”。对熔焊而言，焊缝系指经熔化—凝固后形成的那部分金属。据此定义，熔池及熔池前的待熔化金属都不能称为焊缝。将熔池和待熔化金属看作是焊缝，这与事实相违背。文献[9—11] 证明焊缝不存在压缩塑性应变。图 3b 所示待熔化金属的压缩塑性应变不能算作是焊缝承受的应变。

焊缝应力应变的起点不选在热源正下方的熔池处，即温度场中最高温度连成的抛物线（图 3a 中虚线）的顶端，这是因为此处温度极高，熔池处于过热状态，不可能在此温度下凝固。也就是说此处焊缝尚未形成，也不会有焊缝的应力应变。由于热滞后作用，熔池的凝固要迟到于热源一定距离。熔池凝固首先在熔池边界处而不在熔池中心发生。只有在焊接温度场最高温度连线（图 3a 中虚线）与熔池边界的交点，也是与熔合线的交点，即熔池最宽处才刚

刚开始凝固结晶，也就是说此处才开始形成焊缝，也开始了焊缝应力应变形成过程。或者说焊缝所处的那部分金属，经熔化“退火”，应力应变完全消失后又重新开始产生应力应变，即开始产生焊缝应力应变，故取此断面(图 3a 断面 Ⅱ Ⅰ)作为比较标准和计算焊缝应力应变的起点。由于后面将要提到的原因(焊接残余应力不是压缩塑性应变引起的)，近缝区的压缩塑性应变没有与拉伸塑性应变进行累计。

断面 Ⅲ，Ⅳ，Ⅴ和 Ⅵ的应力应变分布如图 3c，d，e，f 所示，由此可看出冷却过程中的应力应变发展过程，也可看出，焊缝不存在压缩塑性应变。

在文献[11] 中作者有两处错误，在此给以订正。其一是原文图 4c 中应力应变符号标错，正负号颠倒。不过原文的文字叙述是正确的。上述错误是校对疏忽所致，订正后如图 3c 所示。其二是在给出焊缝拉伸塑性应变的公式时，忽略了板端面的缩短平移，即图 1 中的 Δ_l。考虑这一因素，焊缝和近缝区拉伸塑性应变为

$$A\alpha_l(T_0-T_r)-\frac{(R_{rt}-R_{rc})}{E} \qquad (1)$$

式中：A 为焊缝和近缝区以外的金属对其拘束程度不同而引入的系数，略小于 1；α_l 为线膨胀系数；T_0 为断面 Ⅱ 的温度分布；T_r 为室温；R_{rt} 为焊缝中心残余拉应力；R_{rc} 为最大残余压应力；E 为弹性模量。

冷却到室温时焊缝的拉伸塑性应变为

$$A\alpha_l(T_m-T_r)-\frac{(R_{rt}-R_{rc})}{E} \qquad (2)$$

式中：T_m 为熔点温度。

3　关于残余塑性应变

传统观点认为，焊缝存在残余压缩塑性应变[1,3-8]。文献[6] 给出残余压缩塑性应变分布，如图4 中的 B_0KKB_0 所示。

按照文献[6] 的观点，残余压缩塑性应变应是图4 中的 *bcddcbffb* 减去 *KFFKK*，其差值是 *bcddcbg-gb*，如图 5a 阴影部分所示。比较图 4 与图 5a，可看出，B_0KKB_0 与 *bcddcbggb* 明显不同。即残余压缩塑性应变的分布不可能是 B_0KKB_0。

文献[9—11] 指出，焊缝不存在压缩塑性应变。从图 3 也可看出焊缝不存在压缩塑性应变，只有冷却收缩受阻产生的拉伸塑性应变。考虑到焊缝不存在压缩塑性应变，焊缝两侧金属的残余压缩塑性应变分别为 *bcdhigb*，如图 5b 阴影部分所示。如果只考虑冷却过程中产生的拉伸塑性应变，根据文中的计算公式，焊缝和近缝区产生的拉伸塑性应变可以

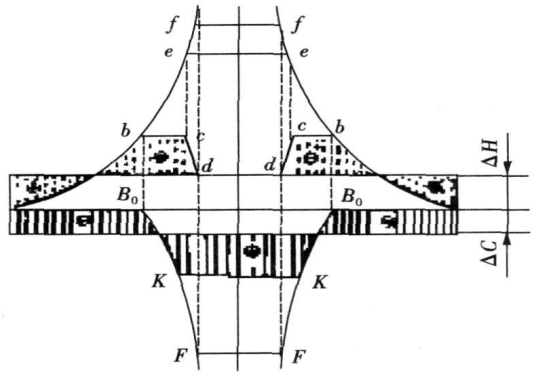

图 4　长板材焊接时的应力应变

Fig 4　Stress and strain distribution in a long welded plate

近似地用熔池最宽处所在断面的温度分布表示，如图 6 所示。该图实际上是图 3f 斜阴影部分的放大。考虑到熔池液态金属能够承受很小的应力，拉伸塑性应变如图 7 所示。比较图 6 与图 4 中的 B_0KKB_0，两者形状类似，但意义却完全不同。其一是图 6 中焊缝和近缝区承受的是拉伸塑性应变，图 4 中的 B_0KKB_0 则为残余压缩塑性应变；其二是图 6 中仅仅焊缝处塑性应变为常量，而图 4 中不仅焊缝而且近缝区塑性应变也为常量。

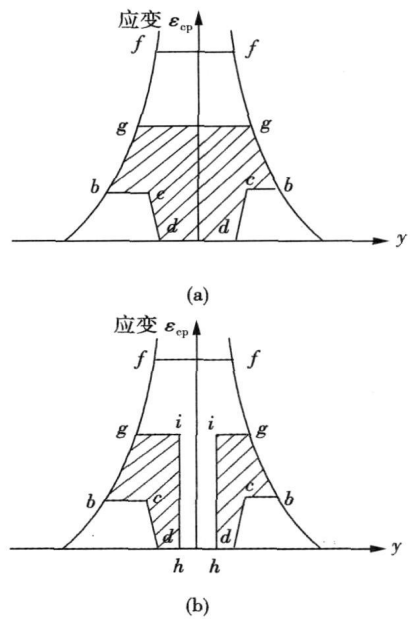

图 5　长板条焊接时的残余压缩塑性应变分布

Fig 5　Residual compressive plastic strain distribution in a long welded plate

近缝区到熔合线的距离不同，加热到的最高温度明显不同，产生的压缩塑性应变也明显不同，在近

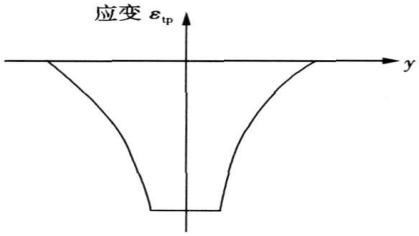

图 6 平板焊接时的拉伸塑性应变分布

Fig. 6 Tensile plastic strain distribution in a welded plate

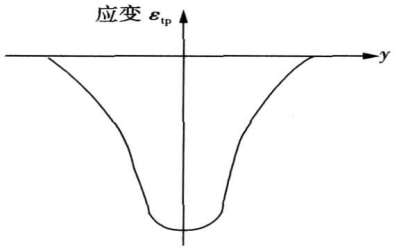

图 7 平板焊接时的拉伸塑性应变分布

Fig. 7 Tensile plastic strain distribution in a welded plate

缝区范围内残余压缩塑性应变不可能是常量。图 8 为实测的钛合金不协调应变即残余压缩塑性应变分布[1]。从图 8 可以看出，在近缝区范围内不协调应变发生急剧变化。比较图 8 与图 4，图 5 可看出，图 4，图 5 所示的残余压缩应变分布是不合理的。

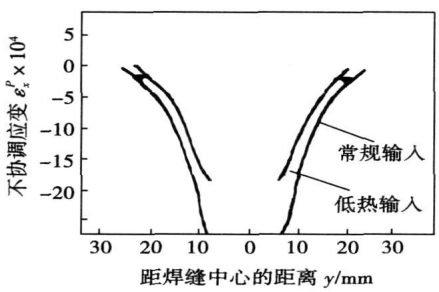

图 8 TA2 钛板氩弧焊的不协调应变分布

Fig. 8 Distribution of incompatible strain during TIG welding for titanium alloy

4 结 论

（1）组成板材的小窄条之间的拘束不可能是完全刚性的，加热时凸出，冷却时凹进，平截面假设不成立。

（2）平截面假设只是分析应力变形时采用的一种手段，提出不用平截面假设照样可以获得类似的焊接残余应力分布。

（3）图 4 B_0KKB_0 所示的残余压缩塑性应变分布的传统观点不成立。焊缝不存在压缩塑性应变，只存在拉伸塑性应变。

（4）提出如图 6，图 7 所示的可以近似用熔池最宽处温度分布表示的拉伸塑性应变分布原理图。焊缝不存在压缩塑性应变，只存在拉伸塑性应变和拉伸弹性应变。焊缝拉伸塑性应变为 $A\alpha_l(T_m - T_r) - (R_{rt} - R_{rc})/E$。

参考文献：

[1] 中国机械工程学会焊接学会. 焊接手册(第三卷)[M]. 2 版. 北京：机械工业出版社，2001.

[2] Masubuchi K. Analytical investigation of residual stresses and distortions due to welding[J]. Welding Journal, 1960, 39(12): 525s—537s.

[3] 奥凯尔勃洛姆 H O. 焊接变形与应力[M]. 雷 原，译. 北京：机械工业出版社，1958.

[4] 关 桥，郭德伦，李从卿. 低应力无变形焊接新技术——薄板构件的 LSND 焊接法[J]. 焊接学报，1990, 11(4): 231—237.

[5] 关 桥，张崇显，郭德伦. 动态控制的低应力无变形焊接新技术[J]. 焊接学报，1994, 15(1): 8—14.

[6] 汪建华，陆 皓. 焊接残余应力形成机制与消除原理若干问题的讨论[J]. 焊接学报，2002, 23(3): 75—79.

[7] 李 菊，关 桥，史耀武，等. 钛合金带热沉钨极氩弧焊中热沉作用[J]. 中国有色金属学报，2004, 14(8): 1301—1307.

[8] 李 菊，关 桥，史耀武，等. 钛合金薄板带热沉钨极氩弧焊的应变场[J]. 材料工程，2004(3): 11—14.

[9] 王者昌. 关于焊接残余应力消除原理的探讨[J]. 焊接学报，2000, 21(2): 55—58.

[10] 王者昌，陈怀宁. 关于焊接应力变形两个问题的进一步探讨[J]. 焊接学报，2002, 23(5): 69—72.

[11] 王者昌. 关于焊接应力变形原理若干问题的探讨[J]. 焊接学报，2006, 27(8): 108—112.

[12] 中国机械工程学会焊接分会. 焊接词典[M]. 北京：机械工业出版社，1998.

作者简介：王者昌，男，1938 年出生，研究员。主要从事钛合金焊接、焊接气孔、焊接热裂纹、焊接力学、堆焊材料和抗磨蚀用钢研究工作。获国家、院、部奖 6 项，获国家发明专利 3 项，参与编审专著 5 部。发表论文 100 余篇。

Email: wanghy@163.com

magnetic field is designed. The simulation result which calculated by finite element code Ansys indicates that radial component exists in arc zone. Applied the longitudinal magnetic field to the process of spray transfer, the movement character of arc and liquid metal jet is obtained by high speed camera. On the basis of electrode magnetic force, the stress of different shaped arc can be analyzed. So the spatial shape of arc is spiral line.

Key words: longitudinal magnetic field; spray transfer; arc shape; electrode magnetic force

Effect of laser-TIG hybrid welding parameters on joint of Mg to steel SHAN Chuang, SONG Gang, LIU Liming (State Key Laboratory of Materials Modification, Dalian University of Technology, Dalian 116024, Liaoning, China). p57—60

Abstract: The lap joining of magnesium alloy AZ31B to steel Q235 by laser-tungsten inert gas (TIG) welding was investigated. The effect of welding parameters on the tensile strength was studied, including laser power, welding speed, laser defocusing amount and current of TIG. It is indicated that the tensile strength of joint increases when the laser power gets higher. But the tensile strength of joint decreases when welding speed gets higher. The current of TIG has nothing to do with the tensile strength. A weld with ideal appearance and good mechanical properties can be obtained with proper process parameters. In the welding process, laser power plays an important role in joining magnesium alloy with steel.

Key words: laser hybrid welding; dissimilar materials; mechanical property

Effect of $ZnCl_2$ and TiO_2 flux on TIG welding of magnesium alloys ZHANG Fan, ZHANG Zhaodong, LIU Liming (State Key Laboratory of Materials Modification, Dalian University of Technology, Dalian 116024, Liaoning, China). p61—64

Abstract: In order to analyze the effect of activating fluxes on the weld bead and the arc shape, activating flux tungsten inert gas (TIG) welding of magnesium alloy has been studied by using single side coated flux and bounded coated flux. It has been found that, the weld penetration with $ZnCl_2$ flux was much deeper than that with TiO_2 flux in both single side coated flux and bounded coated flux TIG welding. For both $ZnCl_2$ and TiO_2 flux, the weld penetration decreased with the increasing flux gap. In the single side coated flux TIG welding, the deflection effect of $ZnCl_2$ flux on molten pool was greater than the one of TiO_2 flux. $ZnCl_2$ flux with low thermal stability changed current channel conductive of the arc, so the arc shape was changed significantly. TiO_2 flux with high thermal stability could not change the current channel conductive of the arc, so the arc shape was not changed significantly.

Key words: magnesium alloy; TIG welding; arc shape; activating flux

Effect of active filler on joining property of silicon carbide to itself by polysilazane LIU Hongli, LI Muqin (School of Materials Science and Engineering, Jiamusi University, Jiamusi 154007, Heilongjiang, China). p65—67

Abstract: Joining of pressureless sintering silicon carbide to itself has been realized using vinyl-containing polysilazane with aluminium nanopowders as joining materials. The joining strength of the joints is strongly affected by adding aluminium nanopowders. Addition of aluminium nanopowders as an active addition can effectively accelerate pyrolysis of polysilazane, lower joining temperature and reduce holes and cracks in the joining interlayer. Therefore it can enhance the joining strength. The maximum bending strength of the joints is 146.8 MPa. This value is obtained at the joining temperature of 1 150 ℃ and after the reinforcement for 2 times. XRD study reveals that the joining material has transformed into an amorphous SiCN ceramic and SiC, Si_3N_4, AlN crystallites. The thickness of interlayer is abaut 5 μm. The joining interlayer is uniform, and the contact at the interfaces is good.

Key words: joining of ceramic; polysilazane(PSZ); active filler; aluminium nanopowders; pressureless sintering silicon carbide

Welding of low-temperature steel 07MnNiCrMoVDR and its low-temperature impact toughness ZHANG Lihong, CHEN Furong (College of Materials Science and Engineering, Inner Mongolia University of Technology, Huhhot 010051, China). p68—72

Abstract: Welding and postweld heat-treatment were carried out for low-temperature steel 07MnNiCrMoVDR. Low-temperature impact toughness was tested, the fiber percentage of fracture at different temperature was calculated, macroscopic and microscopic fracture and microstructure were analyzed for base metal, weld seam and heat-affected zone. The results indicate that impact energy of every zone meets requirement of 07MnNiCrMoVDR steel's mechanical property. It also shows that the chosen welding technology and postweld heat-treatment technology are reasonable. Fiber percentage in base metal fracture is higher than that in heat-affected zone fracture and it is the lowest in welded seam fracture through calculation of fracture's fiber percentage. It indicates low-temperature impact toughness of base metal is the highest, and its is higher in heat-affected zone than that in welded seam.

Key words: welding; low-temperature steel; microstructure; low-temperature impact toughness

Discussion on principle of welding stress and distortion(Ⅰ) WANG Zhechang (Institute of Metal Research, Chinese Academy of Sciences, Shenyang 110016, China). p73—76

Abstract: In the process of heating and cooling during welding, complete rigidity restraint is not in existence between narrow lath of weldment and the face can not keep to be flat which generate convex and concave. While similar welding residual stress distribution can also be obtained without such plain section hypothesis. No residual compressive plastic deformation exists in the weld metal and there is only tension strain. The traditional view that the distribution of residual compressive plastic strain across the weld metal and near its vicinity is not valid. A new schematic sketch of tensile plastic strain distribution is addressed in terms of near temperature distribution at approximate widest location of the molten pool. The size of

tensile plastic strain in the weld metal is $A\alpha_l(T_m - T_r) - (R_{rt} - R_{rc})/E$.

Key words: welding stress and strain; hypothesis of plain section; compressive plastic strain; tensile plastic strain

Influence of TIG dressing on fatigue property of 10Ni5CrMoV steel welded joints XUE Gang, WANG Renfu (Luoyang Ship Material Research Institute, Luoyang 471039, Henan, China). p77—80

Abstract: The fatigue tests were taken on the large angle welded joints of 10Ni5CrMoV steel with and without tangsten inert gas welding(TIG) dressing treatment on the toe. The fatigue life, the relation of load and stroke and the fatigue crack initiation at the same loading condition were analyzed comparatively. The welding residual stress was also measured. The stress field and the strain field of welded joints with and without TIG dressing treatment were calculated by the finite element method. The results indicate that the TIG dressing treatment can improve the fatigue property of the large angle welded joints of 10Ni5CrMoV steel. The fatigue life of the welded joints is increased 34% by TIG dressing on the toe at the same loading condition. The primary cause is that the TIG dressing treatment can improve the weld geometry and reduce the stress concentration on the weld toe. So the stress value in the toe is reduced at the same loading condition and the fatigue ability of the welded joints is increased.

Key words: TIG dressing; 10Ni5CrMoV steel; welded joint; fatigue property

Effect of double-wire narrow gap GMA welding parametars on weld appearance ZHAO Bo, FAN Chenglei, YANG Chunli, ZHANG Liangfeng (1. State Key Laboratory of Advanced Welding Production Technology, Harbin Institute of Technology, Harbin 150001, China). p81—84

Abstracts: The influences of three parameters which are space between wire and edge, space between two wires and angle between two wires on weld appearance were studied in double-wire narrow gap welding with one pool by procedure experiments. The results show that the increase of space between wire and edge can make sidewall penetration and saucer shape of weld surface increase. When the arrangement of wires became parallel, sidewall penetration and saucer shape of weld surface increased to the maximum value. When space between wires increased, sidewall penetration and saucer shape of weld surface increased firstly and then decreased, and finally arrived at peak value when the space between wires is 5—10 mm under the co-action of arc and molten pool energy. But when there was no finger penetration, the three procedure parameters mentioned had little influence on weld penetration. There was lack of fusion of weld bottom when I-shape groove was adopted, and adjusting the three parameters could not eliminate the phenomenon of non-fusion.

Key words: narrow gap welding; twin-wire welding; weld formation

Mechanism and remedy of undercut formation during laser-arc hybrid welding GAO Ming, ZENG Xiaoyan, HU Qianwu, YAN Jun (Wuhan National Laboratory for Optoelectronics, Huazhong University of Science and Technology, Wuhan 430074, China). p85—88

Abstract: To enhance the reliability of laser-arc hybrid welding, undercut formation and its remedy mechanisms during this process were discussed. The results demonstrated that laser can increase undercut critical speed of hybrid welding, which reaches 5 times than that of arc welding with appropriate welding parameters. Two undercut remedying mechanism resulted from laser-arc interaction were found during hybrid welding. The one is the surface tension state of three phases (solid, liquid and gas) at weld toe is changed by laser-arc synergic effects and form a resultant force pointing to the outside of molten pool. The other is the enhancement of flow speed and time of molten metal flowing from pool center to outer by the increasing of heat input and temperature gradient in molten pool. This faster flow drives molten metal to weld toe and avoid undercut, which is the main mechanism for restraining undercut. Furthermore, the experiential formula to undercut critical speed of hybrid welding and the optimal adjusting range of arc voltage were also obtained.

Key words: laser welding; hybrid welding; undercut; critical speed

Numerical simulation of welding residual stress for longitudinal straight weld seam for aluminum alloy thin-wall cylinder ZHOU Guangtao[1], LIU Xuesong[1], YANG Jianguo[1], YAN Dejun[1], FANG Hongyuan[1,2] (1. State Key Laboratory of Advanced Welding Production Technology, Harbin Institute of Technology, Harbin 150001, China; 2. Institute of Astronautical Technology, Shenyang Institute of Aeronautical Engineer, Shenyang 110034, China). p89—92

Abstract: Numerical simulation of TIG welding of thin wall aluminum cylinder by thermo-elastic-plasic FEM was conducted. Based on the generation of analysis model, the values and distribution on the whole cylinder for quasi-steady temperature field and residual stress field were described quantitatively. Experiments were performed to verify the residual stress. It can be drawn that during welding there exits high temperature at the centre of heat source and its vicinity where temperature gradient keeps greater. The longitudinal residual stress in weld seam and its HAZ are tensile, its maximum is in the cross-section at the center of weld length and reached 138 MPa. The maximum compressed transverse residual stress was on the both sides of weld seam. The tensile and compressive region of longitudinal residual stress changed alternately at the circumference of cylinder. The residual stress of the welded Al cylinder has been measured by stress-release method, and excellent agreement between the measured value and calculated value is shown.

Key words: numerical simulation; temperature field; residual stress; stress measurement

Laser welding of new type austenite heat-resistant steel HR3C for ultra supercritical boilers WU Shikai[1], YANG Wuxiong[1], XIAO Rongshi[1], QI Anfang[2], LI Zhongjie[2] (1. Institute of Laser En-